16th World Conference on Earthquake, 16WCEE 2017

Santiago Chile, January 9th to 13th 2017

Paper N° 1991

Registration Code: S-S1462459733

Pseudodynamic Testing of a Precast Structure with Different Configurations of Cladding Panels

M. Lamperti Tornaghi[(1)], P. Negro[(2)]

[(1)] *Scientific Officer, European Commission, Joint Research Centre (JRC), marco.lamperti@jrc.ec.europa.eu*
[(2)] *Senior Scientific Officer, European Commission, Joint Research Centre (JRC), paolo.negro@jrc.ec.europa.eu*

Abstract

The SAFECLADDING Project was aimed at improving the connection systems between cladding panels and precast RC buildings in seismic-prone areas. Three *theoretical approaches* have been assessed: *isostatic*, *dissipative* and *integrated*. They were realized using different *design strategies*, which were represented by several *test setups* within the experimental campaign.

The paper describes the results obtained with two *experimental arrangements*: *horizontal* and *vertical* panels and their comparison with the bare frame, which is the reference for the current design practice that considers panels as non-structural elements. The mock-up was a single-story building, designed for earthquake actions according to the Eurocode 8. The experimental program involved *14* different *setups*, resulting in a total of *37 tests*. All setups were assessed using increasing levels of action, either with *cyclic push-over* test or *pseudo-dynamic* test, the latter both for serviceability and ultimate limit states.

Keywords: Precast Structures, Connections, Cladding Panels, Large Scale Testing, Earthquake Design.

1 Introduction

Precast Reinforced-Concrete (PRC) buildings, together with their connections, maintain their efficiency when adequately designed for earthquake actions [1]. On the contrary, the facade cladding, and mostly the connections with the frame, might meet with failure in the same conditions [2].

The design hypothesis that considers panels as simple masses – without stiffness – can be admissible only with a small interstory drift, where panels and frame coexist without significant interactions. When greater drifts exceed the relative displacement allowed by the clearance, panels act as a part of the seismic resisting system [4]. Connections cannot carry those actions in-plane, thus the fastenings break.

Even assuming that joints are able to sustain so high loads, the reduction of seismic actions for PRC buildings is due to the energy dissipation developed by plastic hinges at the columns base. Unfortunately a large deformation would be needed to activate this mechanism, but the stiffening effect – caused by panels – limits the drift running out the fastening capacity before the development of a large displacement. Therefore, panel joints collapse before exploiting the frame ductility. Different earthquakes occurred over the last years: L'Aquila 2009, Grenada 2010 and Emilia 2012 are only the latter, have validated on field these conclusions [2] [5].

2 The SAFECLADDING research project

The SAFECLADDING Project was conceived to improve the performance of existing PRC buildings, as well as to propose new methods to tackle the above described issues in new buildings.

2.1 Frame-Panels restraint configurations

In cladding systems with *Vertical Panels* (VPs) the gravity action is naturally carried by foundations, hence columns are not affected by vertical loads and they play a role only to avoid the out-of-plane overturning of panels, while horizontal seismic loads are transferred to roof-beams. Conversely, for *Horizontal Panels* (HPs) the gravity force is directly transferred to columns as - in the same manner - the horizontal actions due to earthquake.

The Frame-Panels systems may be sorted as:

Isostatic. The frame deformation-demand is allowed by a relative clearance that uncouples the motion of frame and panels. The two systems are kinematically uncoupled, except for the out-of-plane displacements, Fig.1a.

Integrated. Panels and frame have a coupled motion: the system is kinematically paired, Fig.1b. Panels become part of the seismic resisting system and they act as the main restraint in the horizontal direction, thanks to their higher stiffness. As a consequence, the connections must be adequately over-proportioned to carry the higher loads transferred by the frame according to capacity design.

Dissipative. Specific devices can balance the overall building response, reducing the displacement and keeping the load below an imposed threshold, determined by the connections themselves. Like in the isostatic configuration, the systems are kinematically uncoupled, but they are also constrained by inelastic links, like *friction* [6] or *yielding* [7] [8] devices, Fig.1c. The joints between structure and panels – or among the panels – must be designed to dissipate energy during the earthquake shock [9].

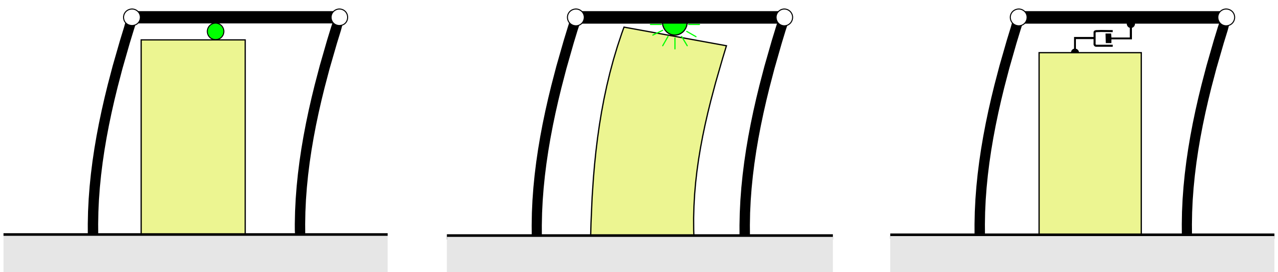

(a) Isostatic (b) Integrated (c) Dissipative

Fig. 1 – Schematic approaches to connect frame and panels: *Restraint Configurations*

2.2 Design Strategies for *Isostatic* and *Dissipative* configurations

Different *Design Strategies* (DS) for the structural system may be chosen. Those are represented by different *test setups* used within the experimental campaign.

ISF. Like an ideal uncoupled system, the *Isostatic Sliding-Frame* presented in Fig.1a is in principle the optimal way to disconnect frame and panels. To achieve this result, VPs are simply leant on the foundation, or better clamped to it, while the relative swaying of the frame must be allowed by a proper connection (slider), which only restrains out-of-plane motions. This hypothesis is typically assumed in the current practice for VPs, while it is impracticable for HPs, because the out-of-plane constraint can not be assured.

DHP. The *Double-Hinged Panel* is the proper way to connect claddings as simple mass without any stiffness contribution. This hypothesis is currently assumed for HPs (Fig.2a) while is uncommon for VPs (Fig.2b), due to the difficulty to realize appropriate base connections. This result may be obtained in VPs either connecting panel edges with hinges, or replacing the top hinge with coupled sliders. HP systems hide other specific features, which are discussed in the following subparagraph.

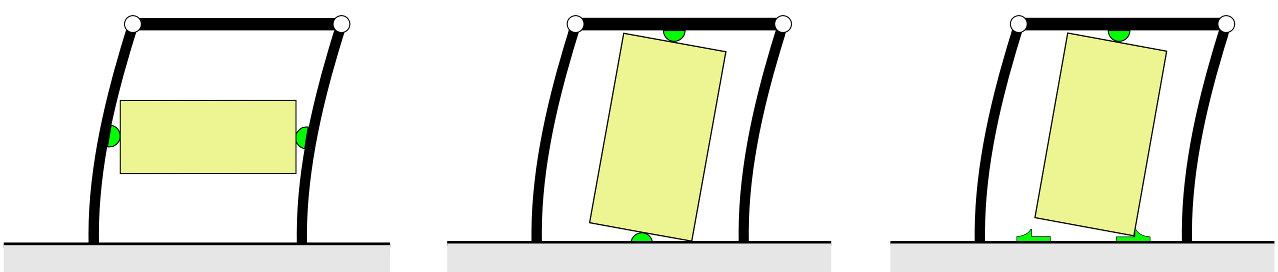

(a) Double-Hinged Panel (HPs) (b) Double-Hinged Panel (VPs) (c) Rocking Panels

Fig. 2 – *Design Strategies* for *isostatic* and *dissipative* configurations

RP. Starting from DHP-VPs, the *Rocking Panel* configuration may be obtained replacing the bottom hinge with a pair of vertical shims. These let the panel free to rock around its bottom corners. Even though this solution looks very similar to the former one, it presents some differences in statics and in kinematic behavior, see Fig. 2c. Despite this solution is not impossible to be used with HPs, it is difficult to be employed in practice.

2.3 Peculiar issues for Horizontal Panels systems

Fastening HPs-cladding to columns alters the overall dynamic response of the building more than VPs. In fact, they changes the mass distribution and increase the stiffness, acting like kinematic restraints between columns.

Whether VPs concentrate the cladding mass at story levels (for a SDOF system, half of seismic mass is on the roof and the rest goes directly on the ground), HPs distribute the mass along columns, which are also joined each other. With the double-hinged panel strategy, the mass of cladding is added without changing the stiffness, as displayed in fig.2a, In this case the columns are already linked by the roof beams. Sometimes one-story buildings with multi-bays facades use additional columns – disconnected from the roof – only to bear panels. In such cases, panels connect columns acting like constraint rods.

Panel-to-Column connections are rarely aligned to the main-axis of panels. In principle it would be better to hang the panel with connections on top. Those connections bear vertical forces, while in some cases horizontal forces are restrained using other devices at panel bottom, see Fig. 3a: *Orthodox approach*, according to prof. *G. Toniolo* [10]). Very often, in the current practice this scheme is overturned: vertical loads are carried by bottom connections while top restrainer control horizontal forces, even out-of-plane, see Fig. 3b. A swift comparison between these two approaches is given by the similarity of the way to hang a picture (Figs. 3a-b).

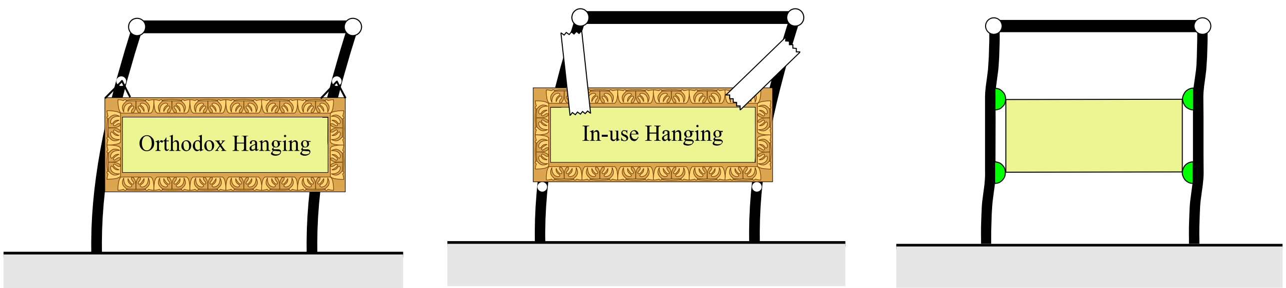

(a) Orthodox hanging (b) In-use hanging (c) Integrated HP hanging

Fig. 3 – Horizontal Panels claddings: schemes of *Design Strategies*

The column stiffness is affected when the panel is fastened with hyperstatic connection: the system becomes fully integrated as in Fig. 3c. The *dissipative configuration* is the combination of an *isostatic configuration* with dissipative devices, such as *Panel-to-Panel* (PtP) connections both for vertical and horizontal panels. With horizontal panels, not rigid devices can be added to restrain horizontal forces by using e.g. *Dissipative Angles* (DA). In the first case, the misalignment of forces between *PtP* connections (both on top and bottom of panels) and the horizontal restraints (only on one side) causes parasitic bending moment, while DAs may be aligned with restrainer on one side only.

In addition, with HPs the lowest panel plays a key role. If it is not connected to the foundation, shear forces must be balanced by columns only. Conversely, if the panel is connected to the foundation, a share of horizontal actions migrates directly to the ground.

2.4 Research objectives

Several issues emerged during the research work carried out by the project partners. Tests on small-scale prototypes and numerical simulations were performed to assess the real behavior and to evaluate the global building response. To detect any hurdles hidden in the path from theory to practice, an extensive experimental campaign was planned on a single full-scale mock-up [12].

Two main *Facade Arrangements* (FA), with HPs and VPs, were selected as the most common in the EU industrial buildings. Furthermore, different connection layouts subdivide each FA into *fourteen setups*. This activity has been entrusted to ELSA, aiming to check the hypotheses, raising potential issues and suggesting improvements, if necessary.

3 Outline of experimental campaign

3.1 The experimental Mock-up

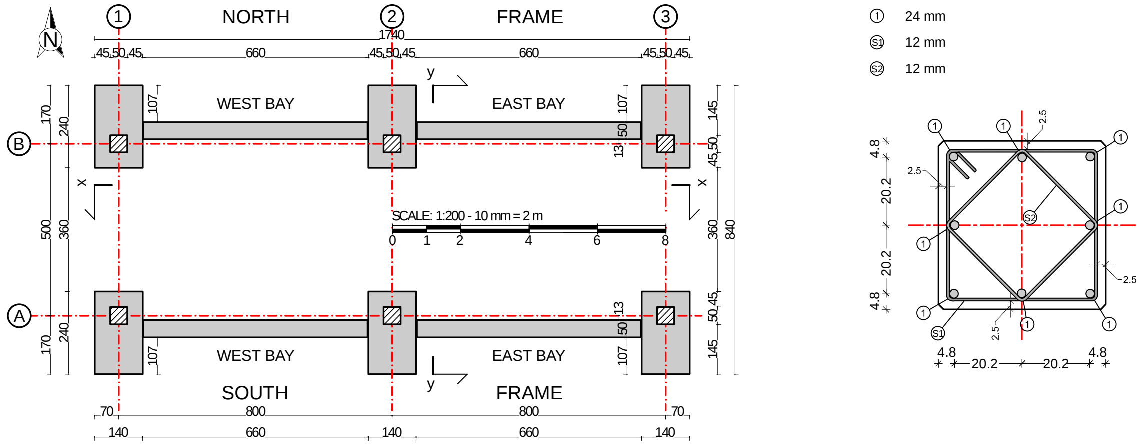

Fig. 4 – Mock-up plan view and base section of columns

All the experiments, the mock-up and the test sequence were designed to assess the most common cladding systems using the same frame structure. The mock-up was a single-story building: 8.13 *m* high, made by two parallel frames (*North* and *South*) which were placed 5.0 *m* from one other, with 8.0 *m* bays (*East* and *West*), as shown in Figure 3 and Figure 4.

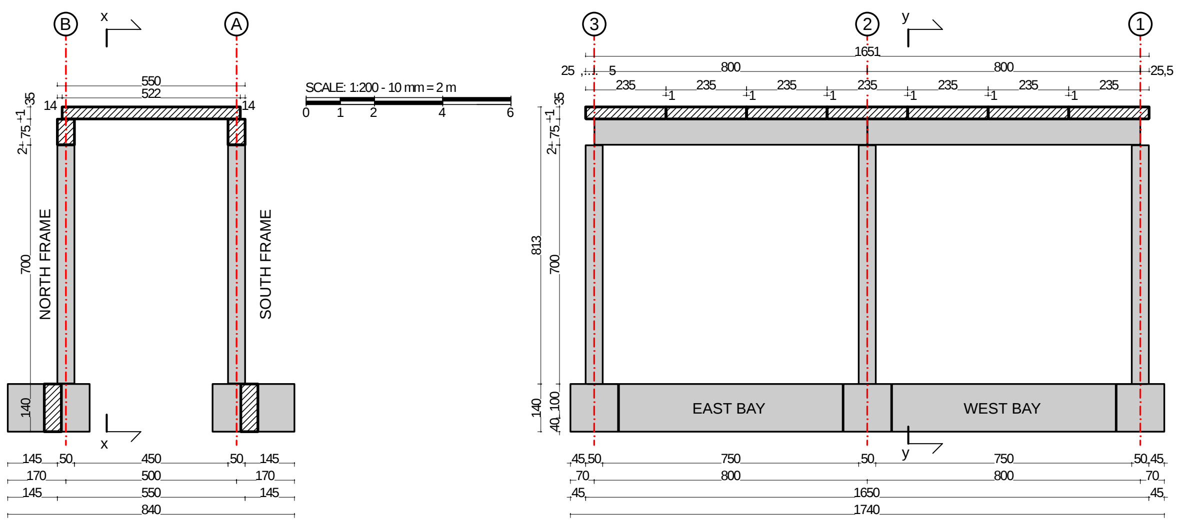

Fig. 5 – Mock-up section *y-y* and *x-x*

Each frame was composed by three square columns, with 500 *mm* side, which were inserted into pocket plinths fastened to the laboratory's strong floor. They were linked to the two foundation beams which were also bearing the panels. Six columns supported the roof beams (750 × 500 *mm*), that in turn carried seven slabs (350 *mm* thick), with masses comparable to common constructions with this typology. The mock-up was designed for seismic actions compatible with the EC8 response spectrum for soil type B. The resulting peak ground accelerations (PGAs) for *Serviceability Limit State* (SLS) is 0.18 *g*, whilst for the *Ultimate Limit State* (ULS) is 0.36 *g*.

3.2 Connections

3.2.1 Panel-to-Frame connections (PtF)

Panel-to-Frame connections, in turn, can be subdivided as follow.

Panel-to-beam joints are used for the vertical panels. Several solutions are readily available on the market, acting as hinges or sliders in the cladding plane, retaining out-of-plane displacements only.

The commercial connections used in this mock-up were in principle certified to act as perfect sliders or shear-keys, used as hinges [15].

Panel-to-column joints are used only for horizontal panels. Connections, commonly available, have been inserted into the mock up columns. Panels vertical load were supported by *bottom corbels* (*in-use* hanging), while overturning and horizontal forces were assured by *shear keys*. The same used as panel-to-beam connection.

An innovative panel-to-column dissipative connection, made by a single *folded plate*, was proposed by *Politecnico di Milano*. The joint is promising both for new constructions and the retrofitting of existing buildings.

Panel-to-foundation joints are not commonly available and, in any case, none of these can be used to create a bottom hinge for vertical panels. In fact friction alone can restrains, the shear action transferred at the panel base could be restrained by friction only for small values of PGA. Introducing FBDs among panels, the equilibrium requires higher shear loads for central-panels, whereas edge-panels are subjected to vertical actions, even opposed to the gravity [13].

RPs may be simply leant on the foundation, eventually using shims to lie them flat. As in the previous case, the equilibrium needs an increase of shear load, that the friction alone could not bear. A special socket was proposed by ELSA to use dissipators with RP setup: the panel is allowed to rock without horizontal sliding.

The integrated system was obtained by clamping the panel into the foundation beam and a commercial connector was employed for this purpose. This consisted of several threadbars for RC, which were screwed to the bottom edge of the panel, then grouted into apposite sleeves within the foundation beam.

With horizontal claddings, an apposite PTFE slider was introduced to uncouple the motion between the lowest panel and the foundation.

3.2.2 Dissipative connections

Several devices have been developed within the Consortium to dissipate energy, either by friction or by yielding. Among the others, only the *Friction-Based Devices* (FBD) [14] and *Dissipative Angles* (DA) have been tested at full-scale on the ELSA mock-up, see Figs.6 and 7.

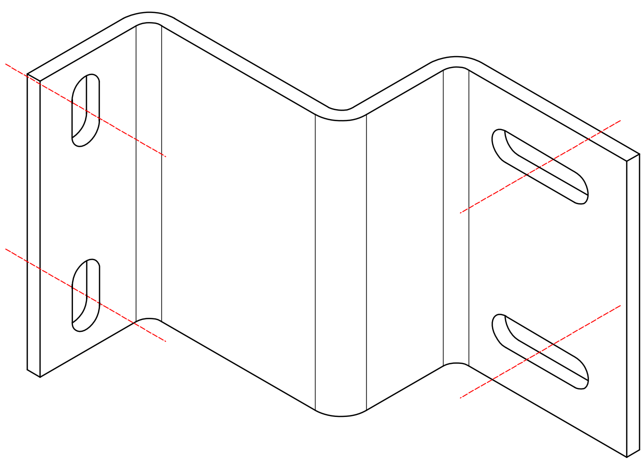

Fig. 6 – Dissipative Angle

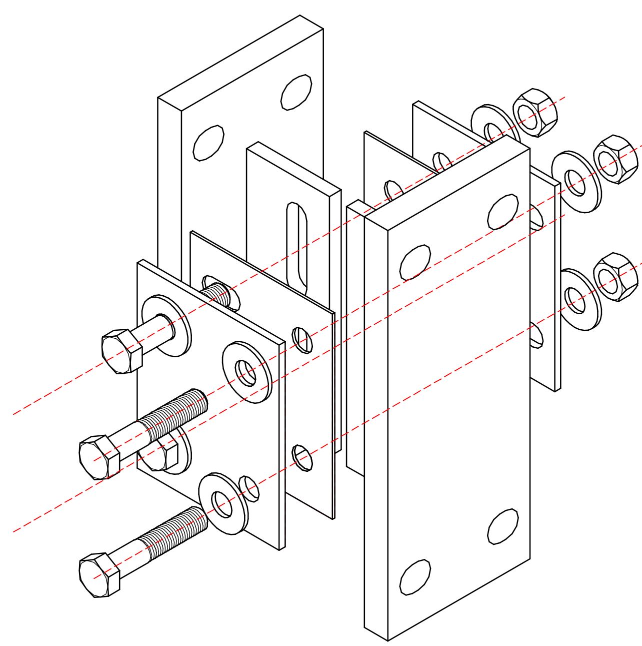

Fig. 7 – Friction-Based Devices

4 Experimental programme

Table 1. summarizes the taxonomy of the experimental campaign. Every setup was tested using increasing levels of action, either with *Cyclic Push-Over* tests (Cyclic PO), or with *Pseudo-Dynamic tests* (PsD). The latter both at *Serviceability Limit State* (SLS) and at *Ultimate Limit State* (ULS).

Table 1 – Taxonomy of the experimental campaign

Arrangement	**Vertical Panels**									**Horizontal Panels**				**Bare Frame**
Restraint Configuration	Dissipative					Isostatic			Integrated	Dissipative			Isostatic	
Design Strategy	DHP				RP	DHP	RP	ISF		DHP			DHP	
Dissipative connections	1FBD	2FBD	3FBD	Sealant	1FBD	none	none	none		2DA	1FBD	2FBD	none	
Test identification	**V1c**	**V1b**	**V1a**	**V2b**	**V2cb**	**V2a**	**V2ca**	**V2d**	**V3a**	**H3b**	**H1c**	**H1b**	**H2a**	**O1a**

4.1 Vertical-Panels arrangement

Three different *restrain configurations* between frame and panels were tested: *Isostatic*, *Integrated* and *Dissipative*. The *isostatic* and the *dissipative* tests were performed, even without PtP connections, using: DHP, RP and ISF test setups. In addition, the dissipative behavior was assessed using an increasing number of FBDs among panels, from one to three. Other tests with a single FBD were also performed with RP setup. In the latter case the tightening was 70% reduced, respect to the other tests, to avoid the edge-panels uplift. After the *isostatic* and the *dissipative* tests, the panels were clamped to the foundation beam to create the *Integrated* restraint configuration.

4.2 Horizontal-Panels arrangement

The vertical panels were then replaced by the Horizontal-Panels arrangement and tested with *dissipative* and *isostatic* RCs. The latter employing both FBDs and DAs, respectively with two setups (1 and 2 FBDs) and with only 2 DAs per panel.

Finally, a sequence of test took place on the *Bare Frame* (BF) only up to a final "*funeral*" test.

Fig. 8 – Layout of Horizontal Panel Arrangement

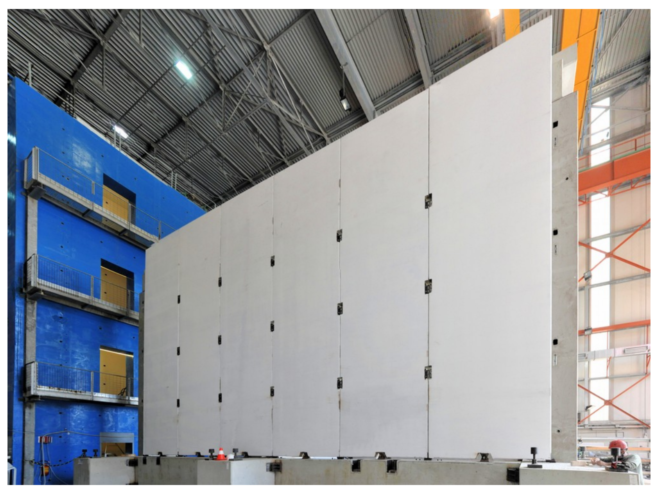

Fig. 9 – Layout of Vertical Panel Arrangement

4.3 Cyclic Push-Over test

In order to assess the real features for each setup, a sequence of cyclic deformations was applied, controlling the top displacement of the structure. Since the frame had to be subjected to dozens of tests, a drift ratio equal to 0.9%, corresponding to a displacement of 63 *mm*, was chosen as the limit of displacement during cyclic tests to avoid excessive damage. At this displacement level the yielding of column base was expected to be safely far. Therefore, the cyclic displacement protocol was composed by seven increasing steps, in turn made of three cycles. The steps followed a 40% increment up to reach of the maximum allowed displacement: 63 *mm*. The displacement steps were thus: ±8.4, ±11.7, ±16.4, ±23.0, ±32.1, ±45, ±63 *mm*.

In addition, the comparison of the results obtained by this test permitted to check the damage of the frame during the whole campaign.

4.4 Pseudo-Dynamic tests

In those tests the equation of motion was formulated in terms of a single degree of freedom, with the roof displacement x parallel to the direction of the excitation at the story's center of mass, which was the *E*-W direction for the mock-up. The computed roof displacement was symmetrically imposed by means of two high-resolution optical encoder displacement transducers, mounted on two reference unloaded frames, and serving each one as feedback for the proportional-integral-derivative (PID) controller [16]. The mass was assumed equal to 170000 *kg* for VPs arrangement and 175000 *kg* for the HPs arrangement.

The reference input motion used in the PsD tests was a unidirectional 12 *s*-long time history, shown in Figure 10 for a PGA of 1.0 *g*. The selected seismic action was represented by a real accelerogram (Tolmezzo 1976) modified to fit the Eurocode 8 (EC8) response spectrum type B for all over the considered frequency interval. Figure 11 illustrates the spectrum of the modified EW component of Tolmezzo record and the EC8 specification. The accelerogram was scaled with reference to the PGS of 0.18 *g* for the *SLS*, and 0.36 *g* for the *ULS*.

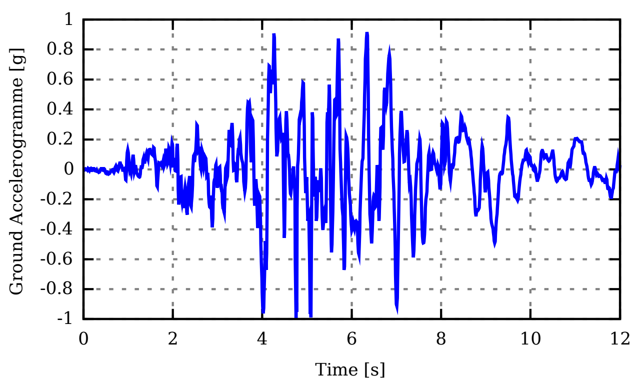

Fig. 10 – Accelerogram time history with PGA = 1.0 g

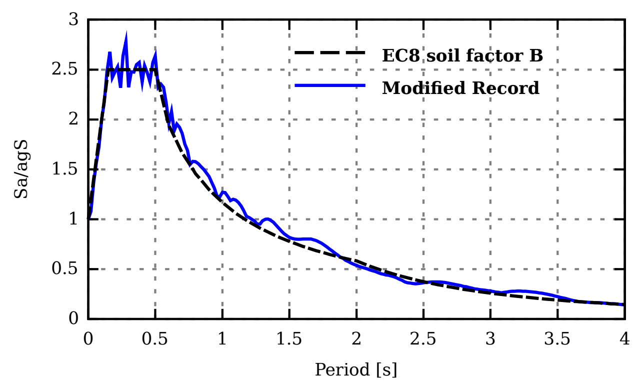

Fig. 11 – Accelerogram and EC8 response spectrum

5 Testing equipment

5.1 Loading system

The displacement on the building roof was imposed by two pairs of hydraulic actuators, which were connected to the ELSA reaction wall. Each jack had 500 *kN* of work load for a total load capacity up to 2000 *kN*. The force was measured by a load cell in each actuator and was transferred to the structure by steel beams, placed along the actuator axes and welded to plates embedded into roof slabs. The drift at roof level was continuously measured by two high-resolution (2 μm) displacement transducers. These *Heidenhain* optical encoders were mounted on two reference frames and serving each one as feedback for the PID controller for each actuators couple.

5.2 Local displacement measures

The local measures of displacements, rotations and deformations were acquired by a scalable network of electrical transducers. A first part of instruments was applied on the bare frame and remaining throughout the whole campaign. During the VPs and HPs arrangements two dedicated layouts of transducers completed the instruments network. A reduction of the measure points was allowed by the double-symmetry of the mock-up. The sensors to measure the panels kinematics were installed only on the *West-bay* of the *South-frame*.

The instruments set-up has been integrated by a camera to capture the displacements of the panels in the *South-frame* (*West-side*), allowing the cross-checking with electrical-transducer measure. Another camera has been used on the *North-frame* (*East-side*) to capture FBDs local motions.

6 Experimental results

All tests performed on the Vertical Panels arrangement (VP) and on the Bare Frame arrangement (BF) are summarized in the Table 2. The results are presented in terms of *maximum displacement* d_{max}, *maximum restoring force* R_{max} and *total dissipated energy* E_d. The following paragraphs present the results of *Cyclic PO Tests* (CPO) performed on Isostatic Restraint Configurations (ISF, DHP and RP), evaluating the effects produced by the use of dissipative devices. Then the results of Pseudo-Dynamic tests (PsD), changing different parameters as restraint configuration (RC), dissipation capacity and earthquake intensity are discussed. Finally, the influence of silicone in sealed joints both in CPO and PsD tests is studied.

The CPO test imposes the same displacement time history to the system, recording the resulting load response. The response comparison, obtained from different isostatic restraint configurations, as well as with dissipative configuration, permits a swift comprehension of the special characteristics of each DS. The kinematic analysis indicates that DHP and ISF are equivalent to the BF, connecting cladding avoiding any stiffness contribution to the frame, as already evidenced by several numerical simulations [12]. The tests on isostatic RC without FBDs are compared in Figures 12a-b.

6.1 Vertical Panels: Isostatic restraint configurations in cyclic PO tests

6.1.1 Comparison between BF, DHP and ISF

The comparison of test results confirms the hypothesis of equivalence between DHP test (V2a-2) and BF test (O1a-0). The two systems are indeed equivalent for d_{max}, R_{max} and *stiffness*. Therefore, thanks to this negligible difference, the DHP setup can be used to install FBDs within the cladding-frame system, enhancing the overall dissipation capacity without adversely affecting dynamic properties.

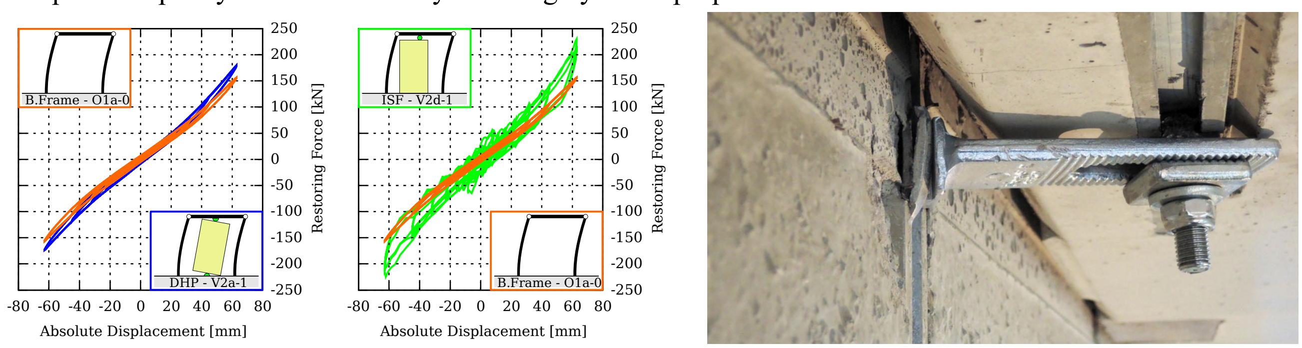

(a) BF and DHP (b) BF and ISF (c) ISF device failure front view – broken channel

Fig. 12 – Comparison among test results of CPO tests: vertical panels with DHP, BF and ISF

On the contrary, the parallel between BF and ISF points out several issues. Indeed, during the ISF test (V2d-1) *two* out of *twenty-four* sliders became *entangled* for the widest displacement series. The following inspection on the connections between the top of the panels and the roof beam, confirmed that the entanglement caused the *failure of the channel-bars* inserted into the panels, Figure 12c. Channel-bars could not be replaced, therefore the scheduled experiments with the same set-up had to be withdrawn. The comparison of results indicates a higher load-gap for the lower displacements, the widest spread reaching 47%. Moreover the Load-Displacement relation shows a wider hysteresis for ISF. The total E_d is more than double compared to the BF.

6.1.2 Comparison between BF, DHP and ISF

The Rocking Panel setup (RP) belongs to isostatic restraint configurations, like the above mentioned cases. It looks very similar to the DHP but – unlike this – the weight of panels is coupled with the frame and acts against its movement. The resulting system is hence statically paired.

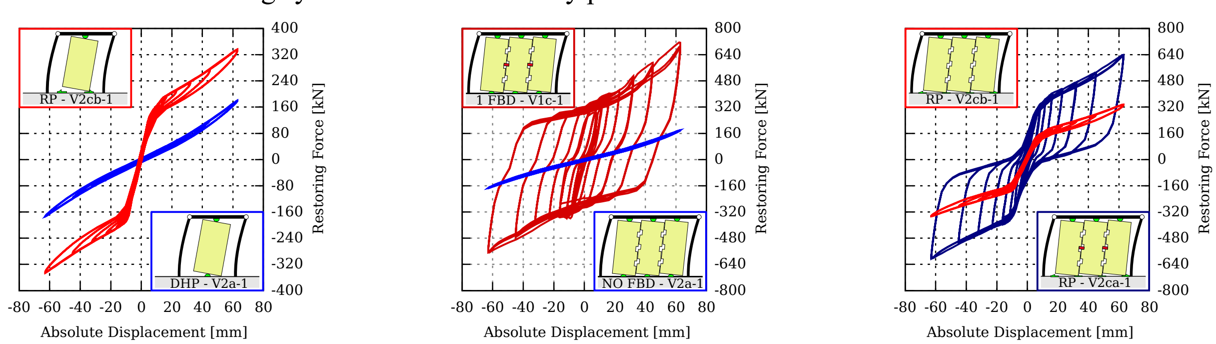

DHP and RP without FBDs DHP with or without FBDs RP with or without FBDs

Fig. 13 – Comparison among test results of CPO tests with and without FBDs: DHP and RP

The L-D diagram of Rocking Panel test (V2cb-1) shows a characteristic bi-linear behavior, with a stiffer central part, which includes the panel uplift, Figure 13b. Once the uplift is overcome, the stiffness decreases becoming comparable to DHP (V2a-1), which represents the columns stiffness only. Indeed, the external branches of the RP test graph have the same slope of DHP test diagram.

The RP setup takes advantage of being self-centering, but this effect was paid with larger loads within the Panel-to-Frame (PtF) connections, +91%. After the V2cb-2 test, a visual survey revealed that the shear-keys were broken in eight out of twelve joints. These connections act as constraints between the top of the panels and the roof beam. Two test repetitions have been performed: V2cb-3 and V2cb-4, to assess whether the problem was related to the RP test itself, or to the damage accumulated during the previous tests. Both these experiments were terminated without any damage in the connections, proving that the RP setup does not cause the failure. In addition, the comparison between the results of the two test series (V2cb-1/V2cb-3 and V2cb-2 /V2cb-4) are comparable. Therefore the damage in the joint did not affected the result.

6.2 Vertical Panels: Pseudo-dynamic tests

The response of each restraint configurations (RC) or design strategy (DS) has been simulated with PsD tests, either using the same setup and same accelerogram with increasing intensity, or using a single input accelerogram changing the test setup. The outputs are finally compared trough the recorded values of load and displacement.

6.2.1 Behavior of FBDs in different Restraint Configurations

The Figure 14 compares the behavior of different RCs each subjected to the ULS earthquake intensity (a_g = 0.36 g), according to the mock-up building design. The comparison here presented involves tests with one FBD, because they were the only ones which were performed both for DHP and for RP. Four kinds of test are considered: *BF*, *Integrated Configuration* (IC), *DHP* and *RP*.

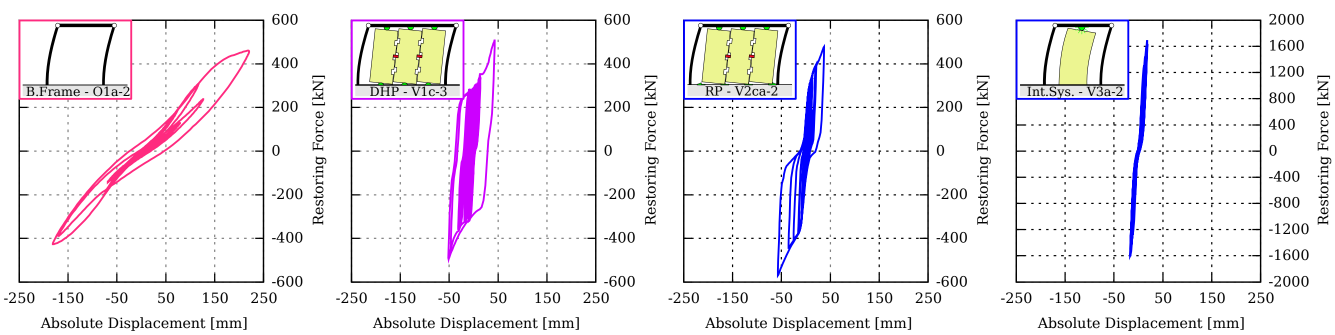

Bare Frame – O1a-2 | DHP with 1 FBD – V1c-3 | RP with 1 FBD – V1b-3 | Integrated – V1a-3

Fig. 14 – Comparison among PsD ULS (0.36 g) tests with different *Restraint Configuration* for VPs

As predicted, the change of arrangement from BF to IC caused the drop of d_{max}, from $d_{max}^{O1a\text{-}2}$ = 220.4 *mm* to $d_{max}^{V3a\text{-}2}$ = 18.43 *mm*, which corresponds to the reduction of 92%. On the contrary, the R_{max} raised by 366%, from $R_{max}^{O1a\text{-}2}$ = 460.2 *kN* to $R_{max}^{V3a\text{-}2}$ = 1683 *kN*. FDBs helped to balance the overall response, reducing the $d_{max}^{V1c\text{-}3}$ = 51.60 *mm* and $d_{max}^{V2ca\text{-}2}$ = 57.15 *mm*. Compared to the BF, they were respectively -77% (DHP) and -72% (RP).

Conversely, the R_{max} was maintained fairly low, close to the BF value: $R_{max}^{O1a\text{-}2}$ = 460.2 *kN*; and the DHP gave 10% more: $R_{max}^{V1c\text{-}3}$ = 507.2 *kN*, whereas RP setup was 23% higher: $R_{max}^{V2ca\text{-}2}$ = 569.8 *kN*.

No damage was discovered during the surveys after each test.

6.2.2 Analysis of connection-failure in the integrated arrangement (test V3a-3)

High *stiffness* combined with low E_d led to the load peak recorded during V3a-2 test. Such a load should be sustained by adequate panel-to-frame connections. Those are not usually designed to be readily replaceable after an earthquake shock, differently from Panel-to-panel connections. Moreover, their defects are not easily detectable. Indeed, even though the survey following the V3a-2 test did not reveal any evidence of damage, the following test V3a-3 ended with the *failure* of *five* out of the *twelve* bolts of the *top hinge joints*. The recorded ultimate load $R_{max}^{V3a\text{-}3}$ = 1780 *kN* was only 5.8% higher than the ULS test $R_{max}^{V3a\text{-}2}$ = 1682 *kN*.

After the failure, an inspection revealed that most of the shear-keys were broken too. A careful comparison reveals that the damage had begun during the previous test. Not the only maximum values of the two tests are comparable, but the plot for the second test lies entirely on the previous one, changing the initial conditions and confirming that the accumulated damage affected the subsequent test. Therefore the bolts had to be already damaged at the end of ULS test (V3a-2).

6.3 Horizontal Panels

The test results on the HPs confirm the main outcomes of VPs tests. The first tests using FBDs were completed without any evident damage. Once again, the results assessed the good performance of dissipative devices (FBDs and DAs) in reducing the maximum displacement while keeping low the maximum load within the system.

During the test H2a-1 a downwards sliding of the panels was observed, demonstrating that the panels of the first row started to support directly those of the second one. A subsequent inspection on the corbel, after the panels removal, revealed the consumption, and in some cases the sway, of the plastic part of the corbel slider. In addition, the four edge columns were evidently cracked near the guides of the shear-keys. Consequently, the scheduled program was continued with the tests of panel-column connections with dissipative angles, withdrawing the scheduled test with rigid angles (*Integrated Configuration*).

6.4 Results of ULS Pseudo-dynamic tests

The comparisons among the maximum recorded displacement in BF, $d_{max}^{O1a\text{-}2} = 220.4\ mm$, with the same values with dissipative devices: 1 FBD, $d_{max}^{H1c\text{-}3} = 52.0\ mm$, and 2 DAs, $d_{max}^{H2b\text{-}2} = 95.1\ mm$, shows again strong reductions, which are respectively -76% and -57%. At the same time, the values of maximum load are quite similar: $R_{max}^{O1a\text{-}2} = 460\ kN$, $R_{max}^{H1c\text{-}3} = 451\ kN$ (-2%), $R_{max}^{H3b\text{-}2} = 417\ kN$ (-9%).

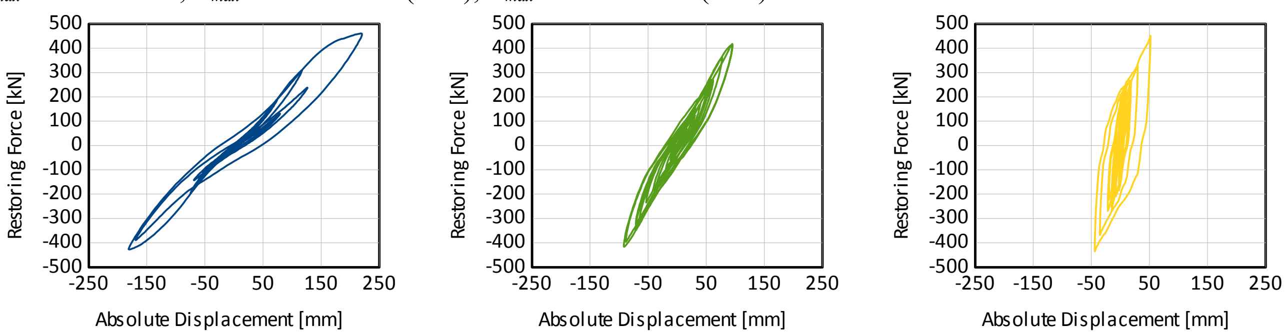

O1a-2 – Bare Frame H3b-3 – Panels with 2DA H1c-3 – Panels with 1 FBD

Fig. 15 – Comparison among PsD ULS (0.36 g) tests with different *Restraint Configuration* for HPs

7 Conclusions

The SAFECLADDING experimental campaign, here presented, tackled the issue of the interaction between cladding panels and frame in precast buildings. Different restraint configurations were used, in turn with several design strategies. All the results have been compared to each other and to the response of the bare frame, which is the reference for the current design practice.

Once again the experimental results confirm that considering panels as simple masses – without stiffness – is far from the real frame-cladding behavior. When the drift exceed the relative displacement, allowed by the clearance, panels become a part of the seismic resisting system, connections cannot carry those actions, thus the fastenings break.

The results of this extensive research confirm that many problems still exist with the current design and construction practice for claddings. On the other hand, many possibilities do exist as for the adoption of other technical solutions, in particular for the use of dissipation. These findings form the basis of new guidelines for claddings which have been recently released by the *SAFECLADDING Consortium* [18] [19].

Table 2 – Summary of the experimental results

#	Test id. ext.	Test id. int.	Connections Panel-to-Frame	Connections Panel-to-Panel	Type of test	Limits	Date	d_{max} [mm]	R_{max} [kN]
1	V1a-1	f01	Vertical Double Hinged Panels	3 FBD	Cyclic PO	0.9% drift	16/10/2014	62.80	1276.42
2	V1a-2	f02			PsD	SLS	17/10/2014	10.87	898.63
3	V1a-3	f03			PsD	ULS	20/10/2014	21.20	1093.8
4	V1a-4	f04			PsD	2.0 ULS (0.72 g)	21/10/2014	46.29	1305.87
5	V1a-5	f05			PsD	2.8 ULS (1.00g)	22/10/2014	87.61	1634.88
6	V1b-1	f06		2 FBD	Cyclic PO	0.9% drift	27/10/2014	62.80	1053.84
7	V1b-3	f07			PsD	ULS	28/10/2014	31.79	691.77
8	V1b-4	f08			PsD	2.0 ULS (0.72 g)	29/10/2014	79.5	1164.39
9	V1c-1	f09		1 FBD	Cyclic PO	0.9% drift	30/10/2014	62.8	715.53
10	V1c-3	f10			PsD	ULS	31/10/2014	51.6	507.2
11	V2a-1	f11		none	Cyclic PO	0.9% drift	03/11/2014	62.8	180.22
12	V2a-2	f12			PsD	SLS (0.10 g)	04/11/2014	59.28	167.04
13	V2b-1	f13		Sealant	PsD	SLS (0.10 g)	17/11/2014	48.17	190.44
14	V2b-2	f14			Cyclic PO	0.9% drift	17/11/2014	62.8	251.85
15	V2ca-1	f15	Rocking Panels	1 FBD	Cyclic PO	0.9% drift	20/11/2014	62.8	637.74
16	V2ca-2	f16			PsD	ULS	21/11/2014	57.15	569.85
17	V2cb-1	f17		none	Cyclic PO	0.9% drift	24/11/2014	62.8	345.5
18	V2cb-2	f18			PsD	SLS	25/11/2014	36.93	244.64
19	V2cb-3	f24			Cyclic PO	0.9% drift	19/01/2015	62.8	344.44
20	V2cb-4	f25			PsD	SLS	20/01/2015	58.06	325.4
21	V2d-1	f19	Isostatic Sliding Frame	none	Cyclic PO	0.9% drift	01/12/2014	62.8	230.08
22	V3a-1	f21	Integrated System	none	PsD	SLS	10/12/2014	8.01	933.54
23	V3a-2	f22			PsD	ULS	11/12/2014	18.43	1682.96
24	V3a-3	f23			Cyclic PO	up to panels failure	12/12/2014	22.9	1780.43
25	H1b-1	g03	Horizontal Double Hinged Panels	2 FBD	Cyclic PO	0.9% drift	17/03/2015	62.80	765
26	H1b-3	g04			PsD	ULS	18/03/2015	41.6	580
27	H1b-4	g05			PsD	1.5 ULS (0.54 g)	19/03/2015	68.6	849
28	H1c-1	g06		1 FBD	Cyclic PO	0.9% drift	20/03/2015	62.80	586
29	H1c-3	g07			PsD	ULS	23/03/2015	52.0	451
30	H2a-1	g08		none	Cyclic PO	0.9% drift	24/03/2015	62.80	275
31	H3b-1	g09		2 DA	Cyclic PO	0.9% drift	23/04/2015	62.80	313
32	H3b-2	g10		2 DA	PsD	SLS	24/04/2015	52.3	250
33	H3b-3	g11		2 DA	PsD	ULS	27/04/2015	95.1	417
34	O1a-0	h01	Bare Frame		Cyclic PO	0.9% drift	05/05/2015	62.80	156.8
35	O1a-1	h02			PsD	SLS (0.10 g)	05/05/2015	64.60	158.6
36	O1a-2	h03			PsD	ULS	06/05/2015	220.4	460.2
37	O1a-3	h06			Cyclic PO	Up to failure	7-8/05/2015	429.8	486.4

8 Acknowledgement

SAFECLADDING is a EU-funded Project Research for SMEs associations (www.safecladding.eu), it was included in the FP7 (Grant Agreement no.314122). *Prof. Giandomenico Toniolo* served as Technical Manager. The executive design of the mock-up and its construction was made by *Styl-Comp S.p.A.*, with the contribution of Mr. *Claudio Pagani* and Mr. *Enzo Ruggeri*. The represented experimental activity was a joint effort of the ELSA technical team.

9 References

[1] Ferrara L, Mola E, Negro P (2006) “Pseudodynamic and cyclic testing of full scale prototypes of precast R/C one storey buildings”, Proceedings of the 1st European Conference on Earthquake Engineering and Seismology, Geneva, September 3-8, 2006.

[2] Bournas D, Negro P, Taucer F (2013) “Performance of industrial buildings during the Emilia earthquakes in Northern Italy and recommendations for their strengthening”, Bulletin of Earthquake Eng.: 1-22, ISSN 1570-761X, http://dx.doi.org/10.1007/s10518-013-9466-z.

[3] Ferrara L, Colombo A, Negro P, and Toniolo G (2004) “Precast vs. cast-in-situ reinforced concrete industrial buildings under earthquake loading: an assessment via pseudodynamic tests” Proceedings of the 13th World conference on earthquake engineering, Vancouver, BC, Canada, 1-6 August, http://www.iitk.ac.in/nicee/wcee/article/13_743.pdf.

[4] Palsson, H., Goodno, B.J. (1988). “Influence of Interstory Drift on Cladding Panels and Connections”, 9th World Conference on Earthquake Engineering (WCEE), Tokyo-Kyoto, Japan, August 2-9, 6, 213-218.

[5] Arnold C, Hopkins D, and Elsesser E. (1987)” Design and Detailing of Architecture Elements for Seismic Damage Control”. Building Systems Development, Incorporated, KRTA Limited and Forell/ Elsesser Engineers, San Mateo, CA.

[6] Maneetes, H. (2007). “Development of a seismic dissipating mechanism for precast concrete cladding panels”, PhD Thesis dissertation, College of Engineering, Pennsylvania State University. http://www.mdpi.com/2075-5309/4/3/418/pdf

[7] Pinelli, J. P., Moor, C., J. I. Craig, and B. J. Goodno (1996). “Testing of Energy Dissipating Cladding Connections” Earthquake Engineering and Structural Dynamics, Vol. 25, 129-147. http://dx.doi.org/10.1002/(SICI)1096-9845(199602)25:2<129::AID-EQE542>3.0.CO;2-0

[8] Pinelli, J.-P., Craig, J. I., Goodno, B. J., and Hsu, C. C. (1993). “Passive Control of Building Response Using Energy Dissipating Cladding Connections” Earthquake Spectra, Vol. 9, No. 3, 529-546. http://dx.doi.org/10.1193/1.1585728

[9] Cohen, J. M. and Powell, G. H. (1993), A design study of an energy-dissipating cladding system. Earthquake Engng. Struct. Dyn., 22: 617–632. doi:10.1002/eqe.4290220706

[10] Prof. Giandomenico Toniolo, private communication in SAFECLADDING meeting, Madrid, April 13^{th} 2015.

[11] Pall, A. S., Marsh, C., & Fazio, P. (1980). Friction joints for seismic control of large panel structures. PCI JOURNAL, 25(6), 38-61.

[12] Dal Lago, Bruno Alberto. "Seismic performance of precast structures with dissipative cladding panel connections" (2015). http://hdl.handle.net/10589/10726.

[13] Biondini, F.; Dal Lago, B. & Toniolo, G. “Role of wall panel connections on the seismic performance of precast structures”, Bulletin of Earthquake Engineering, 2013, 11, 1061-1081, http://dx.doi.org/10.1007/s10518-012-9418-z.

[14] Ferrara, L., Felicetti, R., Toniolo, G., & Zenti, C. "Friction dissipative devices for cladding panels in precast buildings: An experimental investigation." European Journal of Environmental and Civil Engineering 15.9 (2011): 1319-1338. http://dx.doi.org/10.1080/19648189.2011.9714857.

[15] Negro, P., and Lamperti Tornaghi, M., "The Role of Claddings in the Seismic Response of Precast Structures: The SAFECLADDING Full-Scale Tests." Proceedings of the Second European Conference on Earthquake Engineering and Seismology. 2014. http://www.eaee.org/Media/Default/2ECCES/2ecces_ss/756.pdf

[16] Pegon P, Molina F.J, and Magonette G (2008). Saouma, V. & Sivaselvan, M. (Eds.) “Hybrid Simulation: Theory, Implementation and Applications”, Ed. Taylor & Francis, 79-89.

[17] Negro P, Toniolo G (2012) “Design Guidelines for Connections of precast Structures under Seismic Actions”, JRC Scientific and Policy Reports, EUR 25377EN, ISBN 978-92-79-25250-1, http://dx.doi.org/10.2777/37605.

[18] Design guidelines for precast structures with cladding panels; Publications Office of the European Union; ISBN: 978-92-79-58534-0; DOI: 10.2788/956612 http://bookshop.europa.eu/en/design-guidelines-for-precast-structures-with-cladding-panels-pbLBNA27935/

[19] Design guidelines for wall panel connections; Publications Office of the European Union; ISBN: 978-92-79-58533-3; DOI: 10.2788/546845 http://bookshop.europa.eu/en/design-guidelines-for-wall-panel-connections-pbLBNA27934/